Spin transition in the molecular heterospin complex of Cu(hfac)2 with 4,4,5,5-tetramethyl-2-(1-methylpyrazol-5-yl)-4,5-dihydroimidazole-1-oxyl 3-oxide

ARTICLE *in* RUSSIAN CHEMICAL BULLETIN · MARCH 2013

Impact Factor: 0.48 · DOI: 10.1007/s11172-013-0089-y

7 AUTHORS, INCLUDING:

Sergey Fokin

Russian Academy of Sciences

55 PUBLICATIONS **614** CITATIONS

SEE PROFILE

Galina V. Romanenko

Russian Academy of Sciences

312 PUBLICATIONS **1,723** CITATIONS

SEE PROFILE

Artem S. Bogomyakov

Russian Academy of Sciences

155 PUBLICATIONS **618** CITATIONS

SEE PROFILE

Spin transition in the molecular heterospin complex of $Cu(hfac)_2$ with 4,4,5,5-tetramethyl-2-(1-methylpyrazol-5-yl)-4,5-dihydroimidazole-1-oxyl 3-oxide*

S. V. Fokin, E. T. Kostina, E. V. Tret´yakov, G. V. Romanenko, A. S. Bogomyakov, R. Z. Sagdeev, and V. I. Ovcharenko*

International Tomography Center, Siberian Branch, Russian Academy of Sciences, 3a ul. Institutskaya, 630090 Novosibirsk, Russian Federation. Fax: +7 (383) 333 1399. E-mail: fokin@tomo.nsc.ru

The synthesis, structure, and magnetic properties of the products of the reaction for $Cu(hfac)_2$ (hfac is hexafluoroacetylacetonate) with spin-labeled nitronyl nitroxides 4,4,5,5-tetramethyl-2-(1-R-1*H*-pyrazol-5-yl)-3-imidazoline-1-oxyl 3-oxides $L^{5/R}$ (R = Me, Et, Pr, Bu), *viz.*, binuclear complex $[Cu(hfac)_2L^{5/Me}]_2$ and chain polymer complexes $[Cu(hfac)_2L^{5/R}]_n$, are described. The polymer heterospin chains are built according to "head-to-head" (R = Me, Et, Pr, Bu) and "head-to-tail" (R = Pr, Bu) motifs. Compound $[Cu(hfac)_2L^{5/Me}]_2$ is characterized by the ability to reveal the reversible effect of thermally induced spin transition at a temperature about 75 K (without hysteresis). In the set of heterospin Cu^{II} compounds with spin-labeled pyrazoles, this is the earlier unknown example of a molecular complex exhibiting a similar magnetic anomaly.

Key words: molecular magnets, spin transitions, copper(II) complexes, hexafluoroacetylacetonates, nitroxyl radicals, thermomagnetic measurements, X-ray diffraction analysis.

"Breathing" crystals based on heterospin complexes of Cu^{II} hexafluoroacetylacetonate, $[Cu(hfac)_2]$, with stable nitroxyl radicals are valuable objects for the detailed study of structural rearrangements induced by external effects.[1—30] These rearrangements most substantially affect heterospin exchange clusters and result in the appearance of magnetic anomalies in the curves of the effective magnetic moment (μ_{eff}) *vs* temperature.[1—30] The study of coordination compounds $Cu(hfac)_2$ with nitronyl nitroxide radicals containing a pyrazole substituent in position 2 of the imidazoline cycle ($L^{4/R}$) found a whole family of complexes capable of exhibiting effects similar to spin-crossover.[6,10,17,19—21,29,30] They possessed a valuable property: in the most cases, single crystals of the complexes did not crack after passing the temperature range in which the structural phase transition occurred along with the conjugated magnetic transition. Therefore, for all heterospin complexes and related solid solutions,[10,12] the structure at different temperatures (both before and after the magnetic transition) was determined, which presented unique possibility to observe the structural dynamics in these systems in the range of phase transition.

It is noteworthy that the search for similar compounds requires a special approach. The matter is that the stoichiometric nonrigidity of $Cu(hfac)_2$ provokes a potent possibility of formation for a considerable number of compounds by the variation of the synthesis conditions: solvent, temperature, and ratio of reagents. For example, the reaction of $Cu(hfac)_2$ with $L^{4/Me}$ gave 12 crystalline phases, which were structurally characterized. Of them only two phases manifested magnetic anomalies in the $\mu_{eff}(T)$ curve.[11] Therefore, not to "miss" a heterospin phase with nontrivial magnetic properties, one should vary the synthesis conditions and to isolate and study all products formed in the studied synthetic system $Cu(hfac)_2$—radical—solvent. An additional complicating factor is that crystals of two or more solid phases rather than one phase are isolated from the mother liquor. These phases can mechanically be separated in a favorable situation. As for the mentioned products of the reaction of $Cu(hfac)_2$ with $L^{4/Me}$, in several cases, single crystals of different phases were nearly discernible in both color and habitus.[11] Therefore, before a magnetochemical experiment, it was necessary to check each(!) single crystal, and only then this crystal could be joined with crystals of the same phase. Only 5—10 years ago, these circumstances impeded the search for "breathing" crystals and study of their properties. It seems that the discovery of a similar compound was a lucky chance and, as a consequence, a nonclassical spin transition was detected rather rarely.[9] However, to date, when a large experience on the synthesis and magne-

* Dedicated to the Academician of the Russian Academy of Sciences I. P. Beletskaya on the occasion of her birthday.

Published in Russian in *Izvestiya Akademii Nauk. Seriya Khimicheskaya,* No. 3, pp. 0660—0670, March, 2013.

1066-5285/13/6203-661

tochemical analysis of similar objects has been accumulated, it was revealed that this phenomenon is rather popular and nonclassical spin transitions are nor detected even in the case of insignificant structural rearrangements of the heterospin solid phase upon a polymorphous transformation.[7,30]

In this work, we describe the new complex $Cu(hfac)_2$ with the stable nitroxyl radical possessing a spin transition. The complex was observed by the study of a set of heterospin solid phases containing spin-labeled pyrazoles $L^{5/R}$. We also compared the structures and magnetic properties of the $Cu(hfac)_2$ complex with isomeric ligands $L^{4/R}$ and $L^{5/R}$. The comparative analysis showed that the transition from compounds with ligand $L^{4/R}$ to compounds with ligand $L^{5/R}$ leads to a substantial decrease in the plasticity of the crystals and suppression of the "breathing" crystal effect.

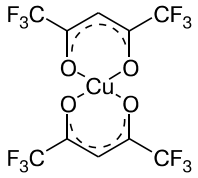

$Cu(hfac)_2$

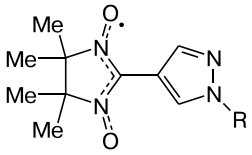

$L^{4/R}$

R = H, Me, Et, Pr, Pr^i, Bu, CD_3

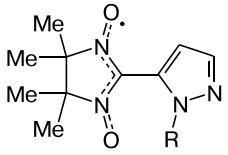

$L^{5/R}$

R = Me, Et, Pr, Bu

Results and Discussion

The synthesis of $L^{5/R}$ was carried out *via* the classical scheme including the preparation of alkylpyrazoles **1a**—**d**, their transformation into bicyclic derivatives **2a**—**d**, and the oxidation of the latter to the target nitronyl nitroxides (Scheme 1).

The structure of $L^{5/R}$ was confirmed by X-ray diffraction analysis. It was found that in molecules of the radicals (Fig. 1) the N—O bond lengths range from 1.272(1) to 1.288(1) Å, which is typical of nitronyl nitroxides.[31,32] In ligand $L^{5/R}$, the angles between the planes of the nitronyl nitroxide fragment CN_2O_2 and pyrazole cycle change from 36.3 to 50.6°, which is significantly higher than in isomeric ligands $L^{4/R}$ (for $L^{4/Me}$, 3.7(3)° (see Ref. 33); for $L^{4/Et}$, 5.4(6)°). Such a substantial increase in the intramolecular dihedral angles in $L^{5/R}$ is a consequence of steric repulsion of substituents R and N—O groups. Already at the first stage of the work, this result suggested that coordination compounds $Cu(hfac)_2$ with $L^{5/R}$ can exhibit more rarely

Scheme 1

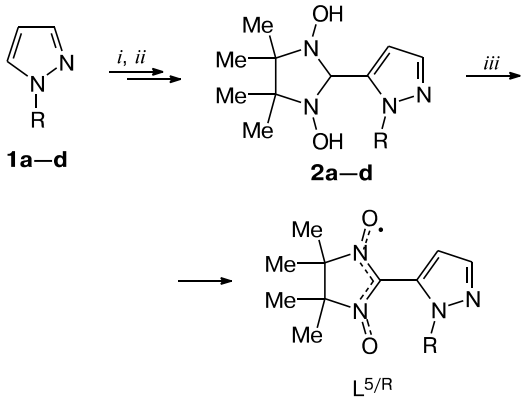

R = Me (**a**), Et (**b**), Pr (**c**), Bu (**d**)

Reagents and conditions: *i*. (1) BuLi, THF, −90 °C, then −10 °C; (2) DMF, −90 °C; (3) HCl, pH = 1; (4) aqueous $NaHCO_3$; *ii*. (1) 2,3-bishydroxylamino-2,3-dimethylbutane sulfate H_2O; (2) $NaHCO_3$. *iii*. $NaIO_4$, CH_2Cl_2, H_2O.

(or do not exhibit at all) effects of nonclassical spin transitions, because ligands $L^{5/R}$ have lower intramolecular "plasticity" compared to their 4/R-isomers, since a possible turning angle of the pyrazole cycle relatively to the 2-imidazoline cycle in $L^{5/R}$ is noticeably larger than in the earlier studied ligands $L^{4/R}$ (see Refs 6, 10, 29, and 30).

The pairs with short distances between O atoms equal to 3.271(3) and 3.313(2) Å can be distinguished in the packings of $L^{5/Me}$ and $L^{5/Pr}$, respectively (see Fig. 1). Their experimental temperature dependences of the effective magnetic moment are well described by the model of exchange-bonded dimers ($H = -2JS_1S_2$).[34] The theoretical processing of experimental data for this model gave the following optimum parameters: $g = 2.03$ and $J = -36.6$ K for $L^{5/Me}$ (see Ref. 33) and $g = 2.05$ and $J = -33.1$ K for $L^{5/Pr}$ (Fig. 2). Chains of radicals with alternating O—O distances of 3.462(1) and 3.593(1) Å can be distinguished in the molecular packing of $L^{5/Et}$; the energy of exchange interactions estimated by the model of exchange-bonded dimers is $J \approx -22$ K. The shortest distance between the O atoms of the NO groups in $L^{5/Bu}$ is 4.553(1) Å, which results in weak exchange interactions between paramagnetic centers ($J \approx -1.4$ K) and, as a consequence, an almost constant value of μ_{eff} in the 10—300 K range (see Fig. 2).

We already mentioned that the reaction of $Cu(hfac)_2$ with nitroxyls can afford a considerable number of heterospin complexes.[11] This turned out valid also for the reaction products of $Cu(hfac)_2$ with $L^{5/R}$. Of the group of isolated compounds, we will concentrate attention only on the complexes with the ratio $Cu(hfac)_2 : L^{5/R} = 1 : 1$, since they are most interesting for the purposes of the present work. These products allow one to compare the

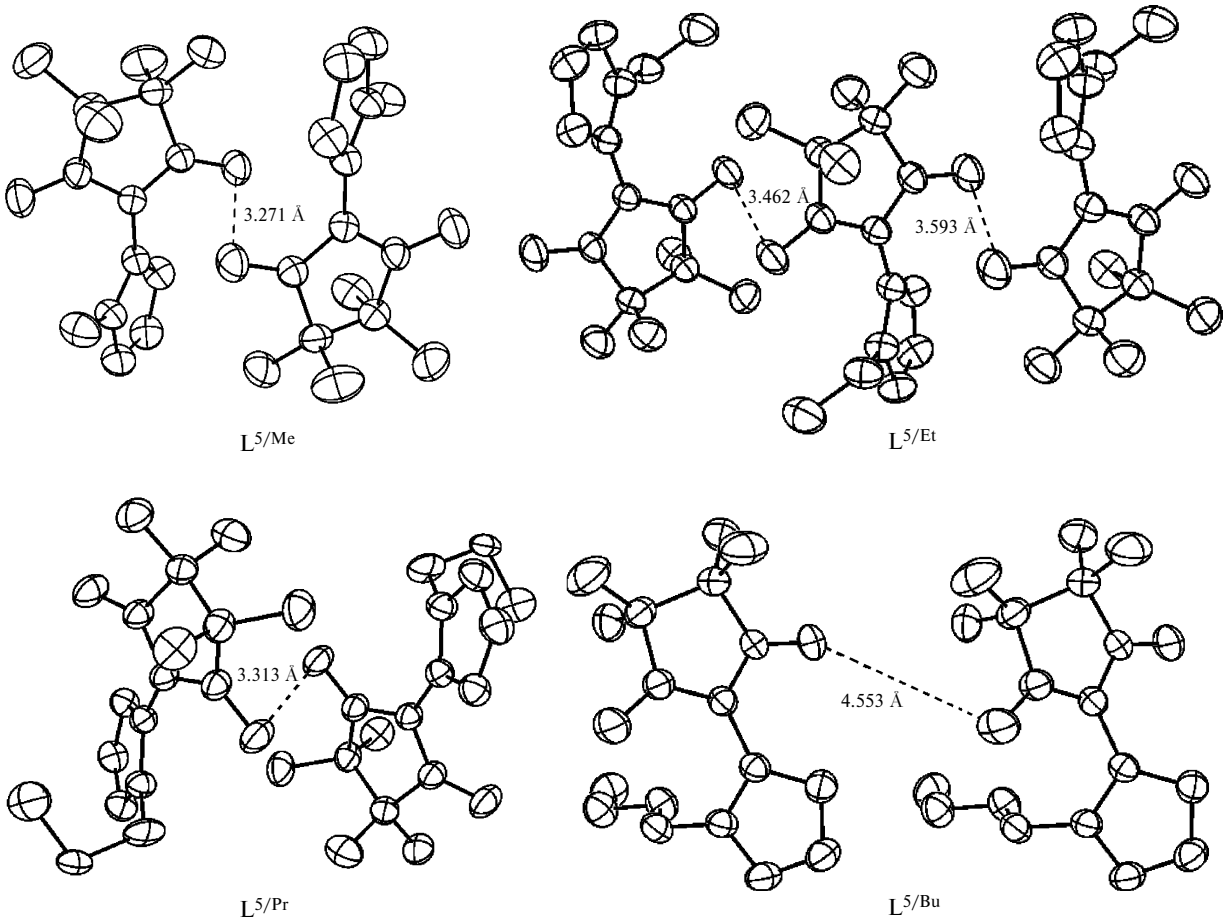

Fig. 1. Structures of molecules $L^{5/R}$ and the shortest intermolecular contacts NO...ON (H atoms are omitted). The parameters of atomic shifts are given with 50% probability.

magnetic structural correlations for the complexes with isomeric $L^{4/R}$ and $L^{5/R}$, because all chain polymers with $L^{4/R}$ exhibiting thermally induced magnetic effect had the composition $[Cu(hfac)_2L^{4/R}]_n$ (see Refs 6, 9, 10, 17, 19, 20, 21, 29, 30).

The procedures of obtaining compounds with the ratio $Cu(hfac)_2 : L^{5/R}$ equal to 1 : 1 in the generalized form are shown in Scheme 2. The reaction of $Cu(hfac)_2$ with $L^{5/Me}$ can produce dimeric complex $[Cu(hfac)_2L^{5/Me}]_2$ and chain polymers $[Cu(hfac)_2L^{5/Me}]_n$. As a rule, they are formed in the synthesis as a mixture of crystals that can be separated mechanically. It was found that $[Cu(hfac)_2L^{5/Me}]_2$ is predominantly formed into the solid phase when using

Scheme 2

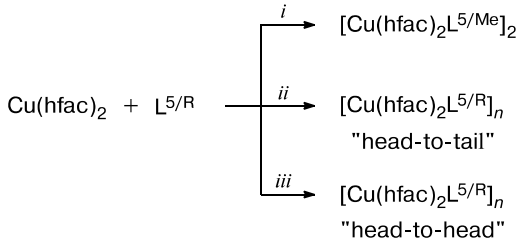

i. R = Me; CH_2Cl_2 : hexane, 3 : 1; *ii*. R = Pr, Bu; hexane; *iii*. R = Me, Et, Pr, Bu; CH_2Cl_2 : hexane, <1 : 1.

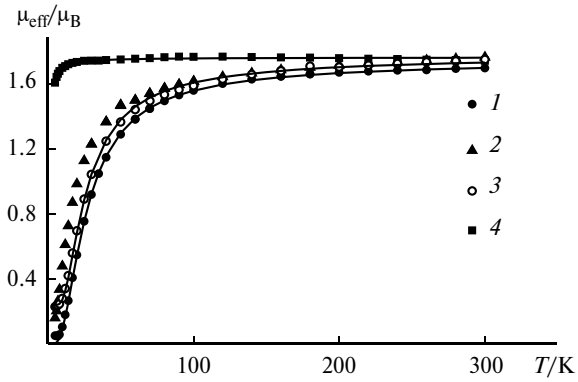

Fig. 2. Plots $\mu_{eff}(T)$ for $L^{5/R}$ at (R = Me (*1*), Et (*2*), Pr (*3*), and Bu (*4*)). Points are experiment, and solid lines are theoretical curves.

CH_2Cl_2—hexane mixture with predomination of CH_2Cl_2, whereas $[Cu(hfac)_2L^{5/Me}]_n$ with a minor admixture of the dimeric complex crystallizes from a mixture with a hexane excess. The solid phases can be obtained only with the use of seeding crystals selected mechanically from mixtures of the complexes.

Product $[Cu(hfac)_2L^{5/Me}]_2$, whose phase consists of centrosymmetric dimeric molecules (Fig. 3), is worth special mentioning. Its structure was determined at 295, 240, 120, and 30 K. Under standard conditions, the coordination modes $CuNO_5$ are elongated octahedra with axial distances Cu—O_{NO} 2.354(2) Å and Cu—O_{hfac} 2.262(2) Å (see Table 1). As the temperature decreases to 120 K, the Cu—O_{hfac} bonds gradually shorten; with the further cooling to 30 K, the complex undergoes the reversible structural phase transition, being a change in the Jahn—Teller axis of the Cu bipyramid (Table 1). As a result, the O_{NO} atom and the O_{hfac} atom in the *trans*-position get in the equatorial plane with Cu—O distances of 2.034(1) and 2.029(1) Å, respectively, and two other O_{hfac} atoms migrate to the axial positions (2.279(1) and 2.320(1) Å).

The character of the dependence $\mu_{eff}(T)$ typical of $[Cu(hfac)_2L^{5/Me}]_2$ (Fig. 4) entirely correlates with the temperature dynamics of the structure. At ambient temperature $\mu_{eff} = 3.45\ \mu_B$, which corresponds to four non-interacting paramagnetic centers with the spin equal to 1/2 and the *g* factor equal to 2. On cooling to ~120 K, μ_{eff} gradually decreases to ~2.85 μ_B and decreases sharply with the further cooling. This is a consequence of the fact that at $T < 120$ K the coordinated O_{NO} atoms transit from the axial to equatorial positions (see Table 1), which results in the appearance of a strong antiferromagnetic exchange in the >N—·O—Cu^{2+} exchange clusters. This effect was described for heterospin dimers $Cu(hfac)_2$ with *meta*-pyridyl-substituted nitronyl nitroxide.[1,2]

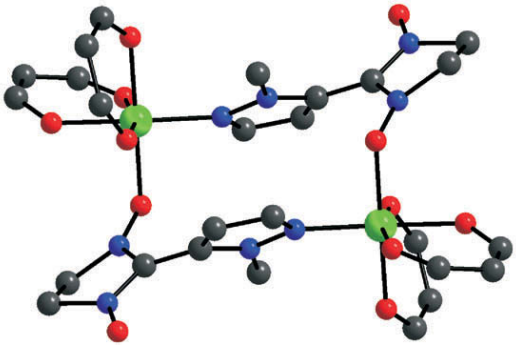

Fig. 3. Structure of dimeric molecule $[Cu(hfac)_2L^{5/Me}]_2$. Hereinafter the CF_3 groups of bischelates $Cu(hfac)_2$ and the CH_3 groups of the 2-imidazoline rings are omitted.*

Table 1. Selected bond lengths in dimer $[Cu(hfac)_2L^{5/Me}]_2$

Bond	*d*/Å			
	30 K	120 K	240 K	295 K
Cu—O_{NO}	2.034(1)	2.227(2)	2.324(2)	2.354(2)
Cu—O_{hfac}	2.029(1)	2.180(4)	2.241(2)	2.262(2)
	2.279(1)	2.101(2)	2.006(2)	1.994(2)
	2.320(1)	2.120(3)	2.012(2)	2.003(2)
	1.980(1)	1.983(2)	1.965(2)	1.973(2)
Cu—N	2.048(2)	2.038(2)	2.019(2)	2.030(3)
N—O	1.320(2)	1.301(3)	1.288(2)	1.289(2)
	1.282(2)	1.281(3)	1.270(2)	1.269(2)
—·O...O·—	3.114(3)	3.172(5)	3.186(3)	3.204(4)

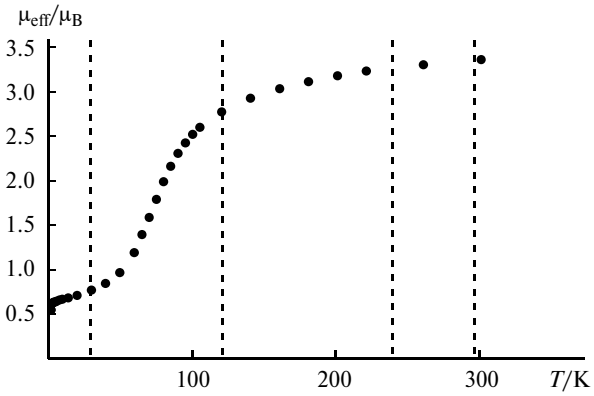

Fig. 4. Plot $\mu_{eff}(T)$ for $[Cu(hfac)_2L^{5/Me}]_2$. Dashed lines show the values of temperature at which the X-ray diffraction study was performed.

Thus, compound $[Cu(hfac)_2L^{5/Me}]_2$ is characterized by the capability of manifesting the reversible effect of the thermally induced spin transition. This effect occur reproducibly and reversibly at temperatures about 75 K on both heating and cooling of the polycrystalline sample of the heterospin complex. No delay in the relaxation of the structure is detected, due to which no hysteresis loop is observed by measurements of the $\mu_{eff}(T)$ dependence. Single crystals of $[Cu(hfac)_2L^{5/Me}]_2$ possess thermal plasticity, which is also a distinctive feature of "breathing" crystals.[10,29]. As in the case of $[Cu(hfac)_2L^{5/Me}]_2$, this makes it possible to determine the structures of both high- and low-temperature phases using the same crystal. The result obtained asserts that compounds capable manifesting the "breathing" crystal effect can be among the heterospin complexes with pyrazol-5-yl derivatives of nitroxyls.

It was also interesting to compare the magnetic structural correlations for the whole series of dimers $[Cu(hfac)_2L^{5/R}]_2$. However, complexes of similar structure ($L^{5/Et}$, $L^{5/Pr}$, and $L^{5/Bu}$), including the conditions favorable for predominant crystallization of $[Cu(hfac)_2L^{5/Me}]_2$, were not detected. All other isolated compounds with the ratio $Cu(hfac)_2 : L^{5/R} = 1 : 1$ had the chain polymer structure (see Scheme 2). Complexes $[Cu(hfac)_2L^{5/R}]_n$ with the "head-to-head" chain motif (Fig. 5) was obtained for

* Figures 3, 5, and 7 are available in full color in the on-line version of the journal (http://www.springerlink.com).

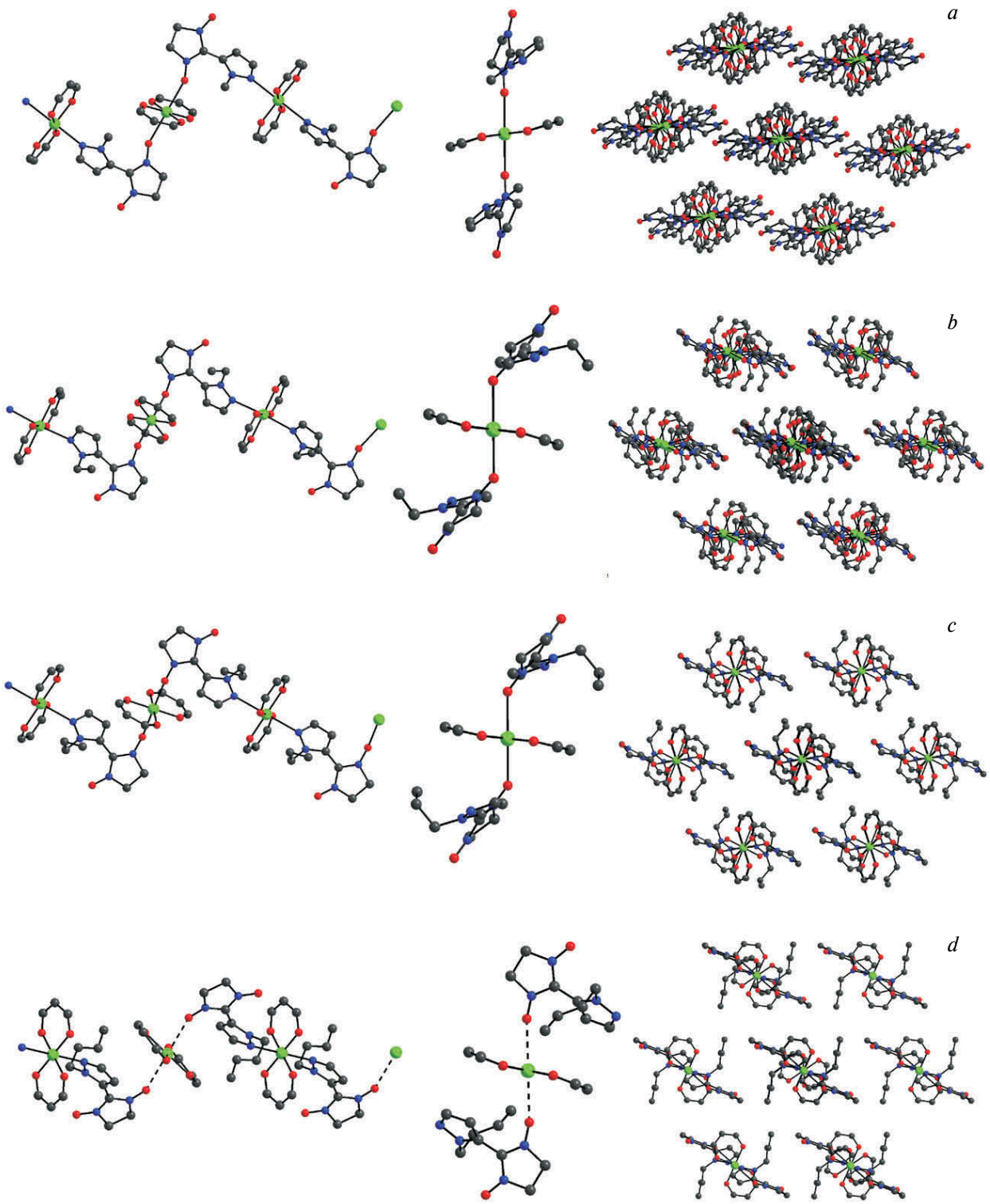

Fig. 5. Fragments of chains with the "head-to-head" motif and their packing in structures $[Cu(hfac)_2L^{5/R}]_n$ (R = Me (*a*), Et (*b*), Pr (*c*), and Bu (*d*)).

all $L^{5/R}$. Two types of coordination modes alternate in the chain: modes CuO_4N_2 in which the square environment of the Cu atom in $Cu(hfac)_2$ is supplemented to distorted octahedral by two N atoms of the pyrazole cycles of two bidentate-bridging $L^{5/R}$ and modes CuO_6 with two O_{NO} atoms of the nitronyl nitroxide fragments in the axi-

Table 2. Selected bond lengths (*d*) in complexes $[Cu(hfac)_2L^{5/R}]_n$ with the "head-to-head" motif of the polymer chain

Bond	*d*/Å					
	$[Cu(hfac)_2L^{5/Me}]_n$			$[Cu(hfac)_2L^{5/(Et)}]_n$ (296 K)	$[Cu(hfac)_2L^{5/Pr}]_n$ (293 K)	$[Cu(hfac)_2L^{5/Bu}]_n$ (240 K)
	28 K	120 K	295 K			
$Cu—O_{NO}$	2.325(2)	2.342(2)	2.374(2)	2.380(2)	2.402(2)	2.711(3)
	2.410(2)	2.408(2)	2.423(2)	2.390(2)		
Cu—N	2.395(3)	2.415(2)	2.450(3)	2.448(2)	2.485(2)	2.448(3)
	2.557(3)	2.586(3)	2.621(3)	2.524(2)		
N—O	1.276(3)	1.272(3)	1.273(3)	1.285(3)	1.288(3)	1.276(3)
	1.282(3)	1.282(3)	1.275(3)	1.277(3)	1.285(3)	1.274(3)
	1.279(3)	1.280(3)	1.279(3)	1.283(3)		
	1.268(3)	1.271(3)	1.270(3)	1.275(3)		
—·O...O·—	3.281(2)	3.346(3)	3.417(3)	3.550(3)	3.458(3)	>5

al positions. The latter are trispin exchange clusters {ONCNO—Cu^{2+}—ONCNO}. The Cu—N and $Cu—O_{NO}$ bond lengths in the coordination modes are within 2.448(2)—2.621(3) and 2.374(2)—2.423(2) Å, respectively (Table 2). In $[Cu(hfac)_2L^{5/Bu}]_n$ the $Cu—O_{NO}$ distance even with a correction to the Jahn—Teller effect noticeably exceeds the upper limit of length for this bond and equals 2.711(3) Å (see Ref. 32). The shortest interchain —·O...O·— contacts were found in $[Cu(hfac)_2L^{5/Me}]_n$ (3.417(3) Å) and $[Cu(hfac)_2L^{Pr}]_n$ (3.458(3) Å).

The experimental dependences $\mu_{eff}(T)$ for this series of solid phases are shown in Fig. 6. In the region of high temperatures, the values of μ_{eff} for these complexes range from 2.6 to 2.7 μ_B, which is close to the theoretical value (2.45 μ_B, at g = 2.00) for the system of almost noninteracting spins of Cu^{2+} ions and nitroxyl based on the empirical formula $\{Cu(hfac)_2L^{5/R}\}$. In $[Cu(hfac)_2L^{5/Bu}]_n$ the distances between the paramagnetic centers are short and, hence, μ_{eff} remains almost unchanged in the range from 20 to 300 K and then begins to decrease. For other complexes and especially for $[Cu(hfac)_2L^{5/Me}]_n$, the temperature decreases results in a decrease in μ_{eff} due to predomination of the antiferromagnetic exchange in the solid phases. Taking into account that the distances between the uncoordinated O_{NO} atoms of the adjacent chains in $[Cu(hfac)_2L^{5/Me}]_n$ are only 3.417(3) Å at 295 K and shorten to 3.281(2) Å on cooling to 28 K (see Table 2), it can be assumed that in the temperature range of 30—300 K the decrease in μ_{eff} is due to the direct exchange interaction between unpaired electrons of the paramagnetic ligands of adjacent chains. A similar situation was observed earlier in the complexes with tetrazolyl- and isoxazolyl-substituted nitronyl nitroxides.[35,36] The strongest antiferromagnetic exchange interactions are manifested by $[Cu(hfac)_2L^{5/Me}]_n$ and $[Cu(hfac)_2L^{Pr}]_n$ in which the —·O...O·— interchain contacts are shortest (see Fig. 6, Table 2).

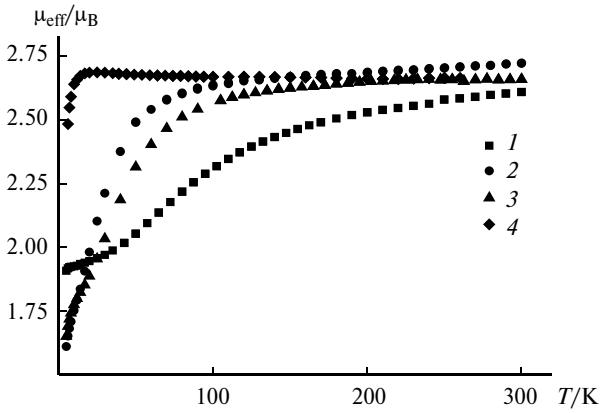

Fig. 6. Plots $\mu_{eff}(T)$ for $[Cu(hfac)_2L^{5/R}]_n$ with the "head-to-head" motif of the polymer chain (R = Me (*1*), Et (*2*), Pr (*3*), and Bu (*4*)).

Chain polymer $[Cu(hfac)_2L^{5/R}]_n$ with the "head-to-tail" motif (Fig. 7) were obtained only for $L^{5/Pr}$ and $L^{5/Bu}$. In their solid phases all coordination modes are the same. The N atoms of the pyrazole cycle and the O_{NO} atoms are localized in vertices of the CuO_5N bipyramids. In the complexes with L^{Pr} and L^{Bu}, the Cu—N distances are 2.411(4) and 2.321(3) Å, respectively, and the $Cu—O_{NO}$ distances are 2.461(4) and 2.549(3) Å, respectively. The —·O...O·— interchain distance are long and exceed 4.5 Å (Table 3).

The $\mu_{eff}(T)$ dependences are similar for the solid phases of $[Cu(hfac)_2L^{5/Pr}]_n$ and $[Cu(hfac)_2L^{5/Bu}]_n$ with the "head-to-tail" motif: at ambient temperature μ_{eff} are 2.72

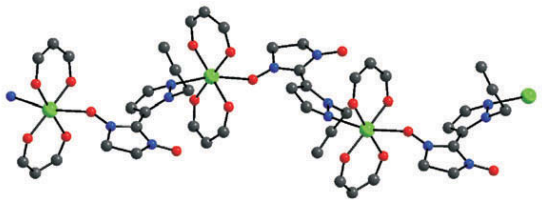

Fig. 7. Fragment of the polymer chain with the "head-to-tail" motif in structure $[Cu(hfac)_2L^{5/Pr}]_n$.

Table 3. Selected bond lengths (d) in $[Cu(hfac)_2L^{5/R}]_n$ with the "head-to-tail" chain motif at 240 K

Bond	d/Å	
	$[Cu(hfac)_2L^{5/Pr}]_n$	$[Cu(hfac)_2L^{5/Bu}]_n$
Cu—O_{NO}	2.461(4)	2.549(3)
Cu—N	2.411(4)	2.321(3)
CuON	147.8(3)	151.1(2)
N—O	1.282(5)	1.278(3)
	1.261(5)	1.280(3)
—·O...O·—	>5	>5

and 2.64 μ_B, respectively, which agrees with the theoretical purely spin value of 2.45 μ_B for two non-interacting paramagnetic centers with spins of 1/2 and g = 2. On cooling μ_{eff} almost does not differ and gradually increases below 100 K, attaining a maximum of 2.9 μ_B at 17 K for $[Cu(hfac)_2L^{5/Pr}]_n$ and at 8 K at $[Cu(hfac)_2L^{5/Bu}]_n$. The $\mu_{eff}(T)$ dependence for $[Cu(hfac)_2L^{5/Bu}]_n$ is shown in Fig. 8 as an example. The long axial distances Cu—O_{NO} (2.461(4) and 2.549(3) Å) in the octahedral $CuNO_5$ modes are a reason for the predomination of the ferromagnetic contribution to the exchange interactions in the >N—·O—Cu^{2+} clusters in the temperature range 25—300 K (see Refs 2, 9, 10, and 25).

Thus, a series of new heterospin complexes similar in structure to the complexes from the family of "breathing" crystals with isomeric nitroxyls $L^{4/R}$ was obtained by the study of the products of the reactions of $Cu(hfac)_2$ with pyrazoles $L^{5/R}$ bearing a paramagnetic substituent in position 5 of the pyrazole cycle. It was established that, unlike the chain polymer complexes with $L^{4/R}$, the solid phases $[Cu(hfac)_2L^{5/R}]_n$ are not characterized by structural rearrangements similar to those obtained in "breathing" crystals with the temperature change. A rare example of the molecular complex $[Cu(hfac)_2L^{5/Me}]_2$ was found, in the solid phase of which the reversible thermally induced transition is observed for the O_{NO} atoms from the axial to equatorial position in the Cu^{II}—O·—N< clusters accompanied by the replacement of weak exchange interaction by strong antiferromagnetic one.

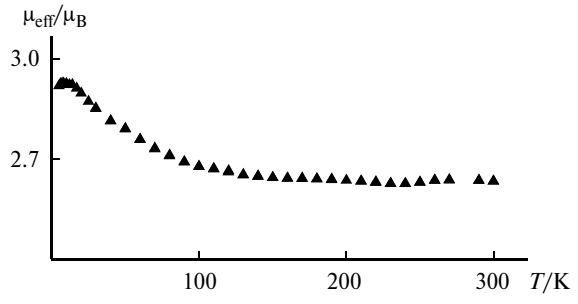

Fig. 8. Plot $\mu_{eff}(T)$ for $[Cu(hfac)_2L^{5/Bu}]_n$ with the "head-to-tail" motif of the polymer chain.

Experimental

1-Ethyl-,[37] 1-propyl-,[6] and 1-butyl-1*H*-pyrazoles,[38] bis(hexafluoroacetylacetonato)copper(II)[39], 2,3-bishydroxylamino-2,3-dimethylbutane and its sulfate salt,[40] and 4,4,5,5-tetramethyl-2-(1-methyl-1*H*-pyrazol-5-yl)-4,5-dihydro-1*H*-imidazole-1-oxyl-3-oxide[33,41] were synthesized using known procedures. Commercial reagents and solvents were used without additional purification.

Plates for TLC (Silica Gel 60 F_{254}, aluminium sheets), silica gel "0.063—0.200 mm, for column chromatography" (Merck), and Al_2O_3 ("pure for chromatography," produced at the Donetsk plant, Ukraine) were used for chromatographic procedures. The IR spectra of samples pressed in KBr pellets were recorded on Bruker VECTOR-22 spectrophotometer. Melting points were determined on BOETIUS microheating stage. Microanalyses were carried out at the N. N. Vorozhtsov Novosibirsk Institute of Organic Chemistry (Siberian Branch, Russian Academy of Sciences) on EURO EA3000 CHNS analyzer. NMR spectra were recorded on Bruker AV-300 (300 MHz for ^{1}H, 75.45 MHz for ^{13}C) and Bruker AV-400 (400.13 MHz for ^{1}H; 100.61 MHz for ^{13}C) instruments at 25—30 °C. The signal from the solvent DMSO-d_6 was used as internal standard: δ_H 2.50, δ_C 39.52. Signals were assigned using the ^{13}C NMR spectra recorded in the *J*-modulation mode (noise proton decoupling, opposite phase for signals from the C atoms with the even number of added protons).

The magnetic susceptibility of polycrystalline samples was measured with an MPMSXL SQUID magnetometer (Quantum Design) in the range from 2 to 300 K in a magnetic field of 5 kOe. Paramagnetic components of magnetic susceptibility χ were determined with allowance for the diamagnetic contribution estimated from Pascal´s constants. Depending on the temperature, the effective magnetic moment was calculated using the formula

$$\mu_{eff}(T) = \left(\frac{3k}{N\mu_\beta^2}\chi T\right)^{1/2} \approx (8\chi T)^{1/2},$$

where N, k, and μ_B are Avogadro´s number, Boltzmann constant, and Bohr magneton, respectively.

X-ray diffraction analysis. Reflection arrays from single crystals were obtained on Bruker AXS SMART APEX II diffractometer equipped with Helix low-temperature attachment (Oxford Cryosystems) and on APEX DUO diffractometer (Cu-Kα radiation for $[Cu(hfac)_2L^{Me}]_2$ at 295 K, Mo-Kα radiation for others; an absorption correction was applied using the Bruker SADABS program, version 2.10). The structures were solved by direct methods and refined by full-matrix least squares in the anisotropic approximation for all non-hydrogen atoms. Positions of H atoms in the most part of structures were calculated geometrically and refined in the riding model. All calculations on structure decoding and refinement were performed using the Bruker Shelxtl Version 6.14 program package. Selected bond lengths in the studied compounds are listed in Tables 1—3. The crystallographic characteristics and experimental details are given in Tables 4 and 5.

2-(1-Ethyl-1*H*-pyrazol-5-yl)-4,4,5,5-tetramethylimidazolidine-1,3-diol (2b). A 2.5 *M* solution of BuLi in hexane (14 mL, 0.035 mol) was added under argon atmosphere (stirred at –90 °C)

Table 4. Crystallographic characteristics and experimental details for compounds $[Cu(hfac)_2L^{Me}]_2$ and $Cu(hfac)_2L^{Me}$

Parameter	Value						
Formula	$[Cu(hfac)_2L^{Me}]_2$				$Cu(hfac)_2L^{Me}$		
M	1429.88				714.94		
T/K	30	120	240	295	28	120	295
Space group	$P2_1/n$	$P2_1/n$	$P2_1/n$	$P2_1/n$	$P\bar{1}$	$P\bar{1}$	$P\bar{1}$
Z	2	2	2	2	4	4	4
a/Å	10.528(2)	10.639(3)	10.6527(17)	10.6980(7)	13.6364(14)	13.7511(18)	13.9588(8)
b/Å	14.634(3)	14.601(3)	14.580(2)	14.6423(10)	14.7625(15)	14.833(2)	14.9820(9)
c/Å	18.653(4)	18.786(4)	18.789(3)	18.8181(12)	15.1325(16)	15.216(2)	15.3531(9)
α/deg	—	—	—	—	64.9660(10)	64.940(2)	64.600(4)
β/deg	102.938(3)	102.674(4)	102.346(11)	102.169(3)	80.335(2)	80.436(2)	80.680(4)
γ/deg	—	—	—	—	87.285(2)	87.077(2)	86.720(4)
V/Å	2800.8(11)	2847.1(12)	2850.7(8)	2881.5(3)	2720.0(5)	2771.8(6)	2861.9(3)
d_{calc}/g cm^{-3}	1.695	1.668	1.666	1.648	1.746	1.713	1.659
μ/mm^{-1}	0.903	0.889	0.887	2.202	0.930	0.913	0.884
I_{hkl}*	18444/4009	21105/4155	21495/6357	35198/5060	13366/7753	21581/7962	23663/12226
R_{int}	0.0300	0.0543	0.0617	0.1091	0.0900	0.0611	0.0499
θ_{max}/deg	23.39	23.47	27.64	67.67	23.30	23.33	28.00
Collection completeness, I_{hkl}	98.0	99.0	95.9	96.7	98.7	99.2	95.5
N	474	505	505	506	823	823	949
Goodness-of-fit	0.893	1.019	0.804	1.025	0.697	0.718	0.835
R_1	0.0241	0.0427	0.0414	0.0464	0.0414	0.0393	0.0420
wR_2 ($I > 2\theta_I$)	0.0644	0.1053	0.0791	0.1332	0.1152	0.1145	0.0782
R_1	0.0257	0.0498	0.1065	0.0486	0.0493	0.0461	0.0878
wR_2	0.0658	0.1094	0.0920	0.1363	0.1253	0.1213	0.0895

* Number of measured/independent reflections.

of 1-ethyl-1*H*-pyrazole (3.0 g, 0.031 mol) in THF (30 mL), and then cooling was ceased. After the temperature was increased to −10 °C, the reaction mixture was again cooled to −90 °C and DMF (3.0 mL, 0.038 mol) was added. The cooling bath was removed. The reaction mixture was stirred for 2 h, concentrated HCl was added to pH ~1, and then the mixture was neutralized with a saturated aqueous solution of $NaHCO_3$. The reaction product was extracted with CH_2Cl_2 (5×10 mL). The joined organic extracts were dried over Na_2SO_4, filtered through silica gel layer (1×5 cm), and evaporated. The residue (3.10 g) containing 1-ethyl-1*H*-pyrazole-5-carbaldehyde was stirred with 2,3-bishydroxylamino-2,3-dimethylbutane sulfate hydrate (4.21 g, 0.016 mol) in water (50 mL) for 10 h. The reaction mixture was treated with $NaHCO_3$ until CO_2 stopped to evolve. The formed product was filtered off, washed with water and toluene, and dried with an air flow. The obtained product was recrystallized from a mixture of EtOAc with heptane. The yield was 1.41 g (18%), finely crystalline white powder. m.p. 194—195 °C. IR, ν/cm^{-1}: 654, 710, 784, 844, 919, 933, 1005, 1029, 1066, 1094, 1122, 1141, 1213, 1237, 1267, 1307, 1375, 1461, 2979, 3014, 3173 br. ^{1}H NMR (DMSO-d_6), δ: 1.04, 1.08 (both s, 6 H each, $C_2(CH_3)_4$); 1.34 (t, 3 H, $CH_2C\underline{H}_3$, J = 7.5 Hz); 4.21 (q, 2 H, $C\underline{H}_2CH_3$, J = 7.5 Hz); 4.75 (s, 1 H, H(2)); 6.23 (s, 1 H, H(3′)); 7.32 (s, 1 H, H(5′)); 7.97 (s, 2 H, NOH). ^{13}C NMR (DMSO-d_6), δ: 15.7 ($CH_2\underline{C}H_3$), 17.4 and 23.8 ($C_2(\underline{C}H_3)_4$), 43.9 (CH_2), 66,4 ($\underline{C}_2(CH_3)_4$), 82.8 (C(2)), 105.0 (C(4′), 137.1 (C(3′)), 142.8 (C(5′)). Found (%): C, 56.4; H, 8.8; N, 22.1. $C_{12}H_{22}N_4O_2$. Calculated (%): C, 56.7; H, 8.7; N, 22.0.

Compounds **2c** and **2d** were synthesized using a similar procedure.

4,4,5,5-Tetramethyl-2-(1-propyl-1*H*-pyrazol-5-yl)-midazolidine-1,3-diol (2c). The yield was 22%, m.p. 159—161 °C. IR, ν/cm^{-1}: 654, 703, 784, 850, 876, 921, 939, 1000, 1028, 1064, 1141, 1159, 1198, 1265, 1302, 1358, 1376, 1388, 1412, 1461, 1496, 2931, 2968, 3186 br. ^{1}H NMR (DMSO-d_6), δ: 0.84 (t, 3 H, $CH_2C\underline{H}_3$, J = 7.5 Hz); 1.01, 1.05 (both s, 6 H each, $C_2(CH_3)_4$); 1.76 (sextet, 2 H, $C\underline{H}_2CH_3$, J = 7.4 Hz); 4.10 (t, 2 H, N—CH_2, J = 7.4 Hz); 4.74 (s, 1 H, H(2)); 6.21 (d, 1 H, H(3′), J = 1.8 Hz); 7.30 (d, 1 H, H(5′), J = 1.8 Hz); 7.92 (s, 2 H, NOH). ^{13}C NMR (DMSO-d_6), δ: 11.2 ($CH_2\underline{C}H_3$), 17.7 and 24.1 ($C_2(\underline{C}H_3)_4$), 23.7 ($\underline{C}H_2CH_3$), 50.9 (N—CH_2), 66.7 ($\underline{C}_2(CH_3)_4$), 83.2 (C(2)), 105.2 (C(4′), 137.4 (C(3′)), 143.5 (C(5′)). Found (%): C, 58.1; H, 8.9; N, 20.9. $C_{13}H_{24}N_4O_2$. Calculated (%): C, 58.2; H, 9.0; N, 21.0.

2-(1-Butyl-1*H*-pyrazol-5-yl)-4,4,5,5-tetramethylimidazolidine-1,3-diol (2d). The yield was 36.8%. ^{1}H NMR (DMSO-d_6), δ: 0.88 (t, 3 H, $CH_2C\underline{H}_3$, J = 7.3 Hz); 1.01, 1.06 (both s, 6 H each, $C_2(CH_3)_4$); 1.27 (sextet, 2 H, $CH_2C\underline{H}_2CH_3$, J = 7.3 Hz); 1.73 (quintet, 2 H, $C\underline{H}_2CH_2CH_3$, J = 7.3 Hz); 4.14 (t, 2 H, N—CH_2, J = 7.25 Hz); 4.74 (s, 1 H, H(2)); 6.21 (d, 1 H, H(3′), J = 1.7 Hz); 7.30 (d, 1 H, H(5′), J = 1.6 Hz); 7.95 (s, 2 H, NOH). Found (%): C, 59.7; H, 9.3; N, 19.8. $C_{14}H_{26}N_4O_2$. Calculated (%): C, 59.5; H, 9.3; N, 19.8.

2-(1-Ethyl-1*H*-pyrazol-5-yl)-4,4,5,5-tetramethyl-4,5-dihydro-1*H*-imidazole-1-oxyl 3-oxide ($L^{5/Et}$). A mixture stirred at 15 °C of **2b** (1.41 g, 5.6 mmol), water (30 mL), and CH_2Cl_2 (30 mL) was added by portions with $NaIO_4$ (1.20 g, 5.6 mmol) for 40 min, and then the reaction mixture was stirred for 1 h. The

Table 5. Crystallographic characteristics and experimental details for compounds $Cu(hfac)_2L^{5/Et}$, $Cu(hfac)_2L^{5/Pr}$, $Cu(hfac)_2L^{5/Bu}$, $L^{5/Et}$, $L^{5/Pr}$, and $L^{5/Bu}$

Parameter	Value							
Formula	$[Cu(hfac)_2L^{5/Et}]_n$	$Cu(hfac)_2L^{5/Pr}$	$[Cu(hfac)_2L^{5/Bu}]_n$	$Cu(hfac)_2L^{5/Pr}$	$[Cu(hfac)_2L^{5/Bu}]_n$	L^{Et}	L^{Pr}	L^{Bu}
Motif	"Head-to-head"			"Head-to-tail"		—	—	—
M	728.97	742.99	757.02	742.99	757.02	251.31	265.34	279.36
T/K	296	293	240	240	240	295	240	240
Space group	$P\bar{1}$	$P\bar{1}$	$P\bar{1}$	$P2_12_12_1$	$P2_12_12_1$	$C2/c$	$P\bar{1}$	$P2_1/c$
Z	4	2	2	4	4	8	2	4
a/Å	14.2918(5)	10.589(5)	10.6490(9)	15.514(2)	10.0469(8)	19.2868(10)	7.9112(5)	7.2487(4)
b/Å	15.3438(5)	11.094(5)	12.0493(9)	19.188(2)	16.1680(13)	7.1455(3)	9.8735(7)	15.9989(9)
c/Å	15.5962(5)	14.089(7)	13.3680(10)	10.355(1)	19.7910(16)	19.8610(10)	10.9848(11)	13.6110(6)
α/deg	62.386(2)	104.42(1)	103.316(6)	—	—	101.356(4)	111.450(5)	101.551(4)
β/deg	80.808(2)	103.79(1)	101.108(6)	—	—	—	93.751(6)	—
γ/deg	82.670(2)	97.67(1)	104.931(6)	—	—	—	113.078(4)	—
V/Å	2985.99(17)	1523.7(12)	1553.8(2)	3082.3(7)	3214.8(4)	2683.5(2)	712.52(10)	1546.51(14)
d_{calc}/g cm^{-3}	1.622	1.619	1.61	1.601	1.564	1.244	1.237	1.200
μ/mm^{-1}	0.849	0.834	0.819	0.824	0.792	0.087	0.086	0.082
I_{hkl}*	48671/13532	16779/7127	25371/7614	15009/7479	27281/7543	11654/3142	15981/4675	17256/4884
R_{int}	0.0858	0.0659	0.0882	0.0837	0.0469	0.0792	0.0431	0.0619
θ_{max}/deg	27.46	28.00	28.37	28.29	27.95	27.98	31.74	30.98
Collection completeness, I_{hkl}	99.0	97.0	97.9	97.9	98.4	96.8	96.4	98.9
N	958	472	482	443	451	240	256	274
Goodness-of-fit	0.752	0.886	0.807	0.729	0.844	0.839	0.694	0.857
R_1	0.0402	0.0436	0.0474	0.0503	0.0409	0.0439	0.0455	0.0452
wR_2 ($I > 2\theta_I$)	0.0721	0.1011	0.1041	0.0861	0.0867	0.0884	0.1404	0.0967
R_1	0.1269	0.0838	0.1407	0.1640	0.0918	0.0877	0.0720	0.0933
wR_2	0.0871	0.1228	0.1270	0.1067	0.0974	0.0993	0.1659	0.1101

* Number of measured/independent reflections.

organic phase was separated, and the aqueous phase was extracted with 10 mL of CH_2Cl_2. Joined organic solutions were dried over Na_2SO_4, filtered through Al_2O_3, and evaporated. The residue was crystallized from hexane. The yield was 0.94 g (67%), dark blue crystals, m.p. 143—144 °C. IR, ν/cm^{-1}: 651, 672, 757, 814, 869, 926, 978, 1043, 1058, 1091, 1147, 1167, 1224, 1272, 1302, 1366, 1385, 1399, 1423, 1460, 1478, 1580, 2941, 2981, 3091, 3121. Found (%): C, 57.4; H, 7.5; N, 22.4. $C_{12}H_{19}N_4O_2$. Calculated (%): C, 57.4; H, 7.6; N, 22.3.

Compounds **$L^{5/Pr}$** and **$L^{5/Br}$** were synthesized using a similar procedure.

4,4,5,5-Tetramethyl-2-(1-propyl-1*H*-pyrazol-5-yl)-4,5-dihydro-1*H*-imidazole-1-oxyl 3-oxide ($L^{5/Pr}$). The yield was 61%, m.p. 101—102 °C. IR, ν/cm^{-1}: 541, 605, 673, 752, 789, 866, 888, 928, 1058, 1137, 1166, 1216, 1277, 1365, 1398, 1419, 1459, 1571, 2877, 2982. Found (%): C, 58.7; H, 8.0; N, 21.3. $C_{13}H_{21}N_4O_2$. Calculated (%): C, 58.9; H, 8.0; N, 21.1.

2-(1-Butyl-1*H*-pyrazol-5-yl)-4,4,5,5-tetramethyl-4,5-dihydro-1*H*-imidazole-1-oxyl 3-oxide ($L^{5/Bu}$). The yield was 67%, m.p. 82—83 °C. IR, ν/cm^{-1}: 541, 610, 656, 677, 731, 760, 804, 866, 885, 926, 1045, 1065, 1134, 1162, 1212, 1264, 1330, 1364, 1383, 1399, 1420, 1453, 1476, 1575, 1686, 1765, 2345, 2876, 2934, 2957, 2995, 3104, 3127 br. Found (%): C, 60.3; H, 8.5; N, 20.4. $C_{14}H_{23}N_4O_2$. Calculated (%): C, 60.2; H, 8.3; N, 20.1.

Bis[μ$_2$-4,4,5,5-tetramethyl-2-(1-methylpyrazol-5-yl)-4,5-dihydro-1*H*-imidazole-3-oxide-1-oxyl-*N*,*O*]-bis(1,1,1,5,5,5-hexafluoropentane-2,4-dionato-*O*,*O*′)dicopper(II) ($[Cu(hfac)_2L^{5/Me}]_2$). A mixture of weighed samples of $L^{5/Me}$ (0.0237 g, 0.1 mmol) and $Cu(hfac)_2$ (0.0477 g, 0.1 mmol) was dissolved in CH_2Cl_2 (3 mL) for 5 min, and 1 mL of hexane was added. The reaction mixture was immediately cooled to −15 °C, and a seeding crystal of the target product was preliminarily added. After 5 days, the dark brown crystals that formed were filtered off, washed with cold hexane, and dried in air. The yield was 0.056 g (80%). Found (%): C, 35.2; H, 2.6; N, 7.8; F, 32.0. $C_{42}H_{38}Cu_2F_{24}N_8O_{12}$. Calculated (%): C, 35.3; H, 2.7; N, 7.8; F, 31.9.

Catena-{bis(μ$_2$-4,4,5,5-tetramethyl-2-(1-methylpyrazol-5-yl)-4,5-dihydro-1*H*-imidazole-3-oxide-1-oxyl-*N*,*O*)-tetrakis(1,1,1,5,5,5-hexafluoropentane-2,4-dionato-*O*,*O*′)-dicopper(II)} ($[Cu(hfac)_2L^{5/Me}]_n$) ("head-to-head"). A mixture of weighed samples of $L^{5/Me}$ (0.0400 g, 0.169 mmol) and $Cu(hfac)_2$ (0.0805 g, 0.169 mmol) was dissolved in 3 mL of CH_2Cl_2, hexane (4 mL) was added, the solution was filtered, and the filtrate was kept in an open flask at 25 °C for 15 min. Then a seeding crystal of the target product was introduced into the solution, and the reaction mixture was kept for 6 h at −15 °C. The formed dark brown crystals were filtered off, washed with hexane, and dried in air. The yield was 0.077 g (65%). Found (%): C, 35.8; H, 2.9; N, 7.6; F, 31.5. $C_{21}H_{19}CuF_{12}N_4O_6$. Calculated (%): C, 35.3; H, 2.7; N, 7.8; F, 31.9.

Catena-{bis(μ$_2$-4,4,5,5-tetramethyl-2-(1-propylpyrazol-5-yl)-4,5-dihydro-1*H*-imidazole-1-oxyl-*N*,*O*)-tetrakis-(1,1,1,5,5,5-hexafluoropentane-2,4-dionato-*O*,*O*′)dicopper(II)}

($[Cu(hfac)_2L^{5/Pr}]_n$) ("head-to-head") was obtained similarly. The yield was 90%. Found (%): C, 37.4; H, 3.1; N, 7.7; F, 31.1. $C_{23}H_{23}CuF_{12}N_4O_6$. Calculated (%): C, 37.2; H, 3.1; N, 7.6; F, 30.7.

Catena-{bis[μ_2-2-(1-ethylpyrazol-5-yl)-4,4,5,5-tetramethyl-4,5-dihydro-1*H*-imidazole-3-oxide-1-oxyl-*N*,*O*]-tetrakis-(1,1,1,5,5,5-hexafluoropentane-2,4-dionato-*O*,*O*´)dicopper(II)} ($[Cu(hfac)_2L^{5/Et}]_n$) ("head-to-head"). A mixture of weighed samples of $Cu(hfac)_2$ (0.0477 g, 0.1 mmol) and $L^{5/Et}$ (0.0252 g, 0.1 mmol) was dissolved in 0.7 mL of CH_2Cl_2. The formed brown solution was diluted with 6 mL of hexane, and the reaction mixture was kept at ambient temperature for 3.5 h and then cooled to −15 °C. After 24 h, the dark green crystals formed were filtered off, washed with hexane, and dried in air. The yield was 0.061 g (85%). Found (%): C, 36.5; H, 2.7; N, 7.6; F, 31.4. $C_{22}H_{21}CuF_{12}N_4O_6$. Calculated (%): C, 36.2; H, 2.9; N, 7.7; F, 31.3. **Catena-{bis[μ_2-2-(1-butylpyrazol-5-yl)-4,4,5,5-tetramethyl-4,5-dihydro-1*H*-imidazole-3-oxide-1-oxyl-*N*,*O*]-tetrakis(1,1,1,5,5,5-hexafluoropentane-2,4-dionato-*O*,*O*´)dicopper(II)} ($[Cu(hfac)_2L^{5/Bu}]_n$) ("head-to-head")** was synthesized similarly. The yield was 60%. Found (%): C, 38.5; H, 3.4; N, 7.3; F, 30.2. $C_{24}H_{25}CuF_{12}N_4O_6$. Calculated (%): C, 38.1; H, 3.3; N, 7.4; F, 30.1.

Catena-{[μ_2-4,4,5,5-tetramethyl-2-(1-propylpyrazol-5-yl)-4,5-dihydro-1*H*-imidazole-3-oxide-1-oxyl-*N*,*O*]-bis(1,1,1,5,5,5-hexafluoropentane-2,4-dionato-*O*,*O*´)copper(II)} ($[Cu(hfac)_2L^{5/Pr}]_n$) ("head-to-tail"). A mixture of weighed samples of $Cu(hfac)_2$ (0.0477 g, 0.1 mmol) and $L^{5/Pr}$ (0.0266 g, 0.1 mmol) was dissolved in 2 mL of hexane at 50 °C. Then the reaction mixture was kept in an open flask at 25 °C for 40 min. The formed needle-like dark green crystals were filtered off, washed with cold hexane, and dried in air. The yield was 0.0676 g (90%). Found (%): C, 37.2; H, 3.1; N, 7.7; F, 30.9. $C_{23}H_{23}CuF_{12}N_4O_6$. Calculated (%): C, 37.2; H, 3.1; N, 7.6; F 30.7.

Catena-{[μ_2-2-(1-butylpyrazol-5-yl)-4,4,5,5-tetramethyl-4,5-dihydro-1*H*-imidazole-3-oxide-1-oxyl-*N*,*O*]-bis(1,1,1,5,5,5-hexafluoropentane-2,4-dionato-*O*,*O*´)copper(II)} ($[Cu(hfac)_2L^{5/Bu}]_n$) ("head-to-tail"). A mixture of weighed samples of $Cu(hfac)_2$ (0.0477 g, 0.1 mmol) and $L^{5/Bu}$ (0.0280 g, 0.1 mmol) was dissolved in 5 mL of hexane at 50 °C. Then the reaction mixture was kept at −15 °C for 24 h. The formed crystals were filtered off, washed with hexane, and dried in air. The yield was 0.0542 g (70%). Found (%): C, 38.4; H, 3.4; N, 7.6; F, 29.2. $C_{24}H_{25}CuF_{12}N_4O_6$. Calculated (%): C, 38.1; H, 3.3; N, 7.4; F, 30.1.

This work was financially supported by the Russian Foundation for Basic Research (Project Nos 11-03-12001, 12-03-00067, 11-03-00027, and 12-03-31028), the Council on Grants at President of the Russian Federation (Program for State Support of Leading Scientific Schools of the Russian Federation and Young Scientists, Project MK-6497.2012.3), the Ministry of Education and Science of the Russian Federation (agreement 8436), the Russian Academy of Sciences, and the Siberian Branch of the Russian Academy of Sciences.

References

1. F. Lanfranc de Panthou, E. Belorizky, R. Calemczuk, D. Luneau, C. Marcenat, E. Ressouche, P. Turek, P. Rey, *J. Am. Chem. Soc.*, 1995, **117**, 11247.
2. F. Lanfranc de Panthou, D. Luneau, R. Musin, L. Öhrström, A. Grand, P. Turek, P. Rey, *Inorg. Chem.*, 1996, **35**, 3484.
3. F. Iwahory, K. Inoue, H. Iwamura, *Mol. Cryst. Liq. Cryst.*, 1999, **334**, 533.
4. A. Caneschi, P. Chiesi, L. David, F. Ferraro, D. Gatteschi, R. Sessoli, *Inorg. Chem.*, 1993, **32**, 1445.
5. M. Baskett, P. M. Lahti, A. Paduan-Filho, N. F. Oliveira, Jr., *Inorg. Chem.*, 2005, **44**, 6725.
6. V. I. Ovcharenko, S. V. Fokin, G. V. Romanenko, Yu. G. Shvedenkov, V. N. Ikorskii, E. V. Tret´yakov, S. F. Vasilevskii, *Russ. J. Struct. Chem.* (*Engl. Transl.*), 2002, **43**, 153 [*Zh. Strukt. Khim.*, 2002, **43**, 163].
7. A. Okazawa, D. Hashizume, T. Ishida, *J. Am. Chem. Soc.*, 2010, **132**, 11516.
8. V. I. Ovcharenko, S. V. Fokin, G. V. Romanenko, V. N. Ikorskii, E. V. Tretyakov, S. F. Vasilevsky, R. Z. Sagdeev, *Mol. Phys.*, 2002, **100**, 1107.
9. P. Rey, V. I. Ovcharenko, in *Magnetism: Molecules to Materials, IV*, Eds J. S. Miller, M. Drillon, Wiley-VCH, New York, 2003, 41.
10. V. I. Ovcharenko, K. Yu. Maryunina, S. V. Fokin, E. V. Tret´yakov, G. V. Romanenko, V. N. Ikorskii, *Russ. Chem. Bull.* (*Int. Ed.*), 2004, **53**, 2406 [*Izv. Akad. Nauk*, *Ser. Khim.*, 2004, 2304].
11. S. Fokin, V. Ovcharenko, G. Romanenko, V. Ikorskii, *Inorg. Chem.*, 2004, **43**, 969.
12. K. Maryunina, S. Fokin, V. Ovcharenko, G. Romanenko, V. Ikorskii, *Polyhedron*, 2005, **24**, 2094.
13. V. I. Ovcharenko, G. V. Romanenko, K. Yu. Maryunina, A. S. Bogomyakov, E. V. Gorelik, *Inorg. Chem.*, 2008, **47**, 9537.
14. M. Fedin, S. Veber, I. Gromov, V. Ovcharenko, R. Sagdeev, A. Schweiger, E. Bagryanskaya, *J. Phys. Chem. A*, 2006, **110**, 2315.
15. M. Fedin, S. Veber, I. Gromov, V. Ovcharenko, R. Sagdeev, E. Bagryanskaya, *J. Phys. Chem. A*, 2007, **111**, 4449.
16. M. Fedin, S. Veber, I. Gromov, K. Maryunina, S. Fokin, G. Romanenko, R. Sagdeev, V. Ovcharenko, E. Bagryanskaya, *Inorg. Chem.*, 2007, **46**, 11405.
17. S. L. Veber, M. V. Fedin, A. I. Potapov, K. Yu. Maryunina, G. V. Romanenko, R. Z. Sagdeev, V. I. Ovcharenko, D. Goldfarb, E. G. Bagryanskaya, *J. Am. Chem. Soc.*, 2008, **130**, 2444.
18. S. L. Veber, M. V. Fedin, G. V. Romanenko, R. Z. Sagdeev, E. G. Bagryanskaya, V. I. Ovcharenko, *Inorg. Chim. Acta*, 2008, **361**, 4148.
19. M. Fedin, V. Ovcharenko, E. G. Bagryanskaya, in *The Treasures of Eureka, I: Electron Paramagnetic Resonance: From Fundamental Research to Pioneering Applications & Zavoisky Award*, Ed. K. M. Salikhov, AXAS Publishing Ltd, Wellington, New Zealand, 2009, 122.
20. M. V. Fedin, S. L. Veber, R. Z. Sagdeev, V. I. Ovcharenko, E. G. Bagryanskaya, *Russ. Chem. Bull.* (*Int. Ed.*), 2010, **59**, 1065 [*Izv. Akad. Nauk*, *Ser. Khim.*, 2010, 1043].
21. M. Fedin, V. Ovcharenko, R. Sagdeev, E. Reijerse, W. Lubitz, E. G. Bagryanskaya, *Angew. Chem., Int. Ed.*, 2009, **47**, 6897.
22. Yu. A. Osip´yan, R. B. Morgunov, A. A. Baskakov, V. I. Ovcharenko, S. V. Fokin, *Physics of the Solid State* (*Engl. Transl.*), 2003, **45**, 1465 [*Fiz. Tverd. Tela*, 2003, **45**, 1396].

23. E. M. Zueva, E. R. Ryabykh, A. M. Kuznetsov, *Russ. Chem. Bull.* (*Int. Ed.*), 2009, **58**, 1654 [E. M. Zueva, E. R. Ryabykh, A. M. Kuznetsov, *Izv. Akad. Nauk*, *Ser. Khim.*, 2009, 1605].
24. A. V. Postnikov, A. V. Galakhov, S. Blügel, *Phase Transitions*, 2005, **78**, 689.
25. S. Vancoillie, L. Rulнљek, F. Neese, K. Pierloot, *J. Phys. Chem. A*, 2009, **113**, 6149.
26. V. A. Morozov, N. N. Lukzen, V. I. Ovcharenko, *J. Phys. Chem. B*, 2008, **112**, 1890.
27. V. A. Morozov, N. N. Lukzen, V. I. Ovcharenko, *Russ. Chem. Bull.* (*Int. Ed.*), 2008, **57**, 863 [V. A. Morozov, N. N. Lukzen, V. I. Ovcharenko, *Izv. Akad. Nauk*, *Ser. Khim.*, 2008, 849].
28. V. A. Morozov, N. N. Lukzen, V. I. Ovcharenko, *Dokl. Phys. Chem.* (*Engl. Transl.*), 2010, **430**, Part 2, 33 [*Dokl. Akad. Nauk*, 2010, **430**, 647].
29. V. I. Ovcharenko, in *Stable Radicals: Fundamentals and Applied Aspects of Odd-Electron Compounds*, Ed. R. Hicks, Wiley-VCH, New York, 2010, 461.
30. G. V. Romanenko, K. Yu. Maryunina, A. S. Bogomyakov, R. Z. Sagdeev, V. I. Ovcharenko, *Inorg. Chem.*, 2011, **50**, 6597.
31. E. V. Tret´yakov, V. I. Ovcharenko, *Russ. Chem. Rev.* (*Engl. Transl.*), 2009, **78** [*Usp. Khim.*, 2009, **78**, 1051].
32. *Cambridge Structural Database*, version 5.33; Cambridge Crystallographic Data Centre: Cambridge, UK, Nov. 2011 (last update May 2012).
33. G. V. Romanenko, S. V. Fokin, S. F. Vasilevskii, E. V. Tret´yakov, Yu. G. Shvedenkov, V. I. Ovcharenko, *Russ. J. Coord. Chem.* (*Engl. Transl.*), 2001, **27**, 360 [*Koord. Khim.*, 2001, **27**, 387].
34. B. Bleaney, K. D. Bowers, *Proc. Roy. Soc. A*, 1952, **214**, 451.
35. E. V. Tret´yakov, S. V. Fokin, G. V. Romanenko, V. N. Ikorskii, A. V. Podoplelov, V. I. Ovcharenko, *Russ. Chem. Bull.* (*Int. Ed.*), 2006, **55**, 66 [*Izv. Akad. Nauk*, *Ser. Khim.*, 2006, 64].
36. S. V. Fokin, S. E. Tolstikov, E. V. Tret´yakov, G. V. Romanenko, A. S. Bogomyakov, S. L. Veber, R. Z. Sagdeev, V. I. Ovcharenko, *Russ. Chem. Bull.* (*Int. Ed.*), 2011, **60** [*Izv. Akad. Nauk*, *Ser. Khim.*, 2011, 2423].
37. J. D. Vaughan, G. L. Jewett, V. L. Vaughan, *J. Am. Chem. Soc.*, 1967, **89**, 6218.
38. V. Ovcharenko, E. Fursova, G. Romanenko, I. Eremenko, E. Tretyakov, V. Ikorskii, *Inorg. Chem.*, 2006, **45**, 5338.
39. J. A. Bertrand, R. I. Kaplan, *Inorg. Chem.*, 1966, **5**, 489.
40. V. I. Ovcharenko, S. V. Fokin, G. V. Romanenko, I. V. Korobov, P. Rei, *Russ. Chem. Bull.* (*Int. Ed.*), 1999, **48**, 1519 [*Izv. Akad. Nauk*, *Ser. Khim.*, 1999, 1539].
41. S. F. Vasilevsky, E. V. Tretyakov, O. M. Usov, Y. N. Molin, S. V. Fokin, Y. G. Shwedenkov, V. N. Ikorskii, G. V. Romanenko, R. Z. Sagdeev, V. I. Ovcharenko, *Mendeleev Commun.*, 1998, 216.

Received June 14, 2012;
in revised form January 28, 2013